Journal of Metallic Material Research | Volume 04 | Issue 02 | October 2021

BILINGUAL PUBLISHING CO.
Pioneer of Global Academics Since 1984

Journal of Metallic Material Research
https://ojs.bilpublishing.com/index.php/jmmr

ARTICLE

Surface Tension of GaInSnBiZn Liquid High-entropy Alloy

Shirong Zhu Lu Liu Qiaoli Lin[*]

State Key Laboratory of Advanced Processing and Recycling of Non-ferrous Metal, Lanzhou University of Technology, Lanzhou, 730050, China

ARTICLE INFO

Article history
Received: November 12 2021
Accepted: December 10 2021
Published Online: 15 December 2021

Keywords:
High-entropy alloy
Pendant-drop method
Thermodynamics
Formation entropy

ABSTRACT

As an emerging alloy material, high-entropy alloy has potential applications that distinguish it from traditional alloys due to its special physicochemical properties. In this work, a low melting point GaInSnBiZn high-entropy alloy was designed based on Miedema model, and its surface tension was measured by the continuous pendant-drop method. The results show that the intrinsic surface tension of GaInSnBiZn high-entropy alloy at 80 °C is 545±5 mN/m, and the surface tension of the liquid alloy is significantly reduced by the formation of surface oxide film. The surface tension of GaInSnBiZn high-entropy alloy was analyzed by using theoretical models (Guggenheim model, GSM (general solution) model and Butler model), and the thermodynamic characteristics of the surface tension formation were further verified by combining with thermodynamic calculations, among which the calculated results of Butler model were in good agreement with the experimental data. Meanwhile, it is found that the surface concentration of Bi in the alloy is much larger than the nominal concentration of its bulk phase, which contributes the most to the surface tension of the alloy, however, it contributes the least to the entropy of the alloy formation in combination with the Butler model.

1. Introduction

Surface tension is a fundamental physical property of liquid materials and its magnitude determines the conduct of many production processes, such as joining, electronic packaging, and forming [1,2]. On the other hand, high-entropy alloys, as an emerging multi-component alloy material, have shown impressive potential applications with their unique physicochemical properties under extreme conditions [3-6]. Therefore, mastering the surface/interfacial properties of liquid high-entropy alloys is of great research importance to expand their further applications.

For the measurement of surface tension of liquid metals, it mainly involves the general means such as the sessile-drop method, the pendant-drop method, the maximum bubble pressure method, and the droplet oscillation method. Each method has its own advantages and disadvantages, for

---

*Corresponding Author:
Qiaoli Lin,
State Key Laboratory of Advanced Processing and Recycling of Non-ferrous Metal, Lanzhou University of Technology, Lanzhou, 730050, China;
Email: lqllinqiaoli@163.com

DOI: https://doi.org/10.30564/jmmr.v4i2.4091

example, the sessile-drop and pendant-drop methods require a smaller amount of liquid compared to the maximum bubble pressure method, and the droplet oscillation method requires magnetic levitation or microgravity conditions and is much less accurate than the sessile-drop and pendant-drop methods [7-9]. In the case of liquid metals, the oxidizable nature of the surface (except for inert noble metals) can easily lead to small apparent values or even to surface tension values without any physical significance, regardless of the method used. For this reason, in most cases, surface tension measurements on liquid metals are generally performed under controlled atmospheres, such as high vacuum (ultra-high vacuum), inert atmospheres (argon or helium), or even reducing atmospheres (hydrogen), which makes the implementation of surface tension measurements extremely inconvenient. Once the oxide film is formed on the liquid metal surface, a fresh liquid metal surface can be obtained by forming a pendant drop by mechanical extrusion, which allows the original liquid metal surface oxide film to be removed. Since the formation of the oxide film on the liquid metal surface takes a certain amount of time, even at the fastest it takes at least 0.02 seconds [10]. The formation of hanging drops by continuous extrusion of the liquid metal and its capture using a high-speed camera makes it a possibility to measure the surface tension of liquid metals under the atmosphere. It is well known that the mixing Gibbs free energy ($G^{\mathrm{mix}}=H^{\mathrm{mix}}-TS^{\mathrm{mix}}$) of high entropy alloys (HEA) is mainly derived from the contribution of mixing entropy to the formation of the alloy, so the mixing enthalpy of the alloy is as close to zero or positive as possible, and the more complex the component, the higher the entropy value ($S^{\mathrm{mix}}=R\ln N$, where R is the gas constant and N is the number of alloy components). Meanwhile, the multi-component composition of high-entropy alloys poses difficulties for the theoretical prediction of surface tension, and the typical surface tension characteristics of high-entropy alloys cannot be reliably related to thermodynamic parameters.

In this work, a low melting point GaInSnBiZn high entropy alloy is designed based on the Miedema model. As a new low melting point liquid metal, it is expected to have potential applications in chip and thermal management devices and liquid metal printed circuits through the characterization of its thermal properties and the study of field phenomena and effects.

2. Alloy Design and Preparation

The mixing enthalpies of the binary alloys based on the Miedema model, as shown in Table 1, are positive except for the In-Sn and In-Bi binary systems, and both In-Sn and In-Bi mixing enthalpies are close to positive values. the binary phase diagram of In-Sn indicates the presence of solid solution without intermetallic compound formation; the binary phase diagram of the In-Bi system indicates the possible presence of both BiIn, Bi_3In_5 and $BiIn_2$ intermetallic compounds with melting points of 110 °C, 88.9 °C and 89.5 °C, respectively, where $BiIn_2$ has a mutual transformation with the solid solution of In containing Bi at 49 °C [11]. From the enthalpy of formation of ternary alloys, there is no ternary compound for alloy formation. Therefore, the GaInSnBiZn alloy mixed in equal proportions satisfies the thermodynamic conditions for the formation of a high entropy alloy.

The GaInSnBiZn high-entropy alloy was obtained from pure metal sheets with purity of Ga ≥ 99.999%, Bi ≥ 99.999%, In ≥ 99.999%, Sn ≥ 99.99%, and Zn ≥ 99.99%, respectively, which were cut and placed in corundum crucible and heated to 425 °C under high vacuum (10^{-3} Pa) for half an hour, and then cooled rapidly. The GaInSnBiZn high-entropy alloy was further characterized by metallographic analysis (Keyence, VHX-900, Japan) to determine the microstructural characteristics and simultaneous thermal analysis (Netzsch, STA 449, Germany) to determine the melting point and possible phase transitions. The kinetic process of oxide film generation on liquid metal surfaces was characterized by laser (wavelength 632.8 nm) ellipsometry (Sentech, SE 400adv-PV, Germany).

Table 1. Mixing enthalpy and formation enthalpy of alloys in binary and ternary systems

Binary systems	$\Delta H^{mix\quad i}_{in\,j\,or\,j\,in\,i}$, kJ/mol
Ga-In	10.177, 11.983
Ga-Sn	3.239, 4.035
Ga-Bi	14.342, 20.011
Ga-Zn	0.064, 0.054
In-Zn	14.193, 10.117
In-Sn	−1.415, −1.488
In-Bi	−4.738, −5.582
Sn-Bi	4.808, 5.384
Sn-Zn	5.272, 3.578
Bi-Zn	22.764, 13.796
Ternary systems	ΔH^{f}, kJ/mol
Ga-In-Sn	2.077
Ga-In-Bi	3.484
Ga-In-Zn	3.944
Ga-Sn-Bi	4.169
Ga-Sn-Zn	1.359
Ga-Bi-Zn	5.980
In-Sn-Bi	0.229
In-Sn-Zn	2.198
In-Bi-Zn	3.444
Sn-Bi-Zn	4.238

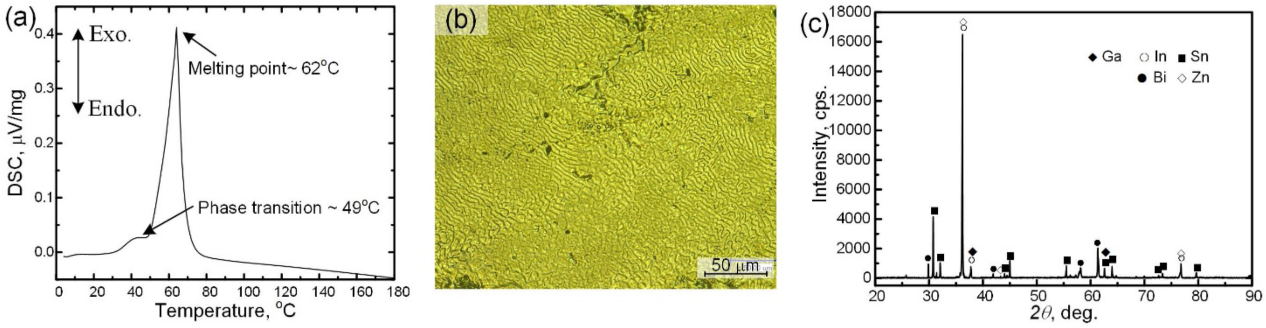

Figure 1. Physicochemical properties and microstructures of GaInSnBiZn high-entropy alloy
(a) DCS results; (b)Typical microstructures; (c) XRD spectrum

The GaInSnBiZn alloy after melting was ramped up to 180 °C at 5 °C/min for simultaneous thermal analysis. As shown in Figure 1a, an endothermic peak appeared at 49.6 °C, which according to the phase diagram corresponds to the temperature point at which the phase transition between $BiIn_2$ and In solid solution with Bi; an obvious endothermic peak appeared at 62.4 °C, which corresponds to the melting point of the alloy. The typical metallographic microstructures are shown in Figure 1b, with a relatively homogeneous microstructures and no segregation generation. The XRD pattern of the alloy after solidification (shown in Figure 1c), no obvious solid solution or intermetallic compounds could be identified after the formation of the alloy.

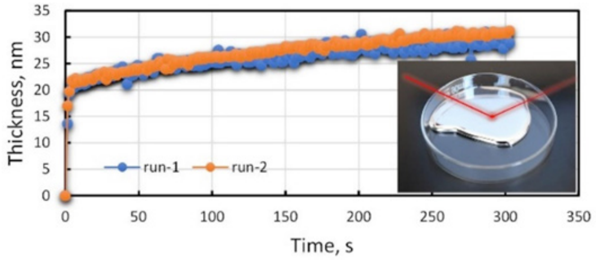

Figure 2. Variation of oxide film thickening with time of GaInSnBiZn high-entropy alloy

When the GaInSnBiZn alloy was melted at a constant temperature platform (constant temperature of 80 °C), the oxide film was scraped off with a ceramic sheet and the laser ellipsometer was applied, setting the laser incidence angle to 75°, and the complex refractive index and absorption coefficient were measured as 1.0422 and 6.4159, respectively. After being exposed to atmosphere for 5 min, the measured complex refractive index and absorption coefficient were 1.2644 and 6.1039, respectively. Based on this, after repeated in-situ measurements, the variations of oxide film thickening were obtained, is shown in Figure 2. The oxide film can be completely covered in about 2 s. Subsequently, the oxide film thickening shows a slow growth in logarithmic form with thickness variation between 20-30 nm, and even after 24 h, the oxide film thickness on the liquid metal surface is still about 40 nm, reflecting the good passivation effect of the oxide film. Based on the above results, the application of high-speed continuous extrusion to form hanging drops (at a rate of about 20 ms/drop), even under atmospheric atmosphere, is sufficient to obtain a clean, oxide film-free surface for measuring the intrinsic surface tension of liquid metals.

3. Surface Tension Measurement

The reliability of this method of measurement was first verified by recording continuous droplet squeeze drops by high-speed camera. The eutectic Ga-In alloy (E-GaIn, eutectic point of 16 °C, density 6.280 g/cm^3) was used for the study, and the outer diameter of the drop tube used was 0.46 mm. as shown in Figure 3a, the Young-Laplace curve matched well with the shape of the droplet profile, and the surface tension obtained was 623.1 mN/m (where the measurement error was $(1.79\text{-}2.23) \times 10^{-3}$ mN/m), which is in agreement with the literature [12]. E-GaIn alloys are oxidation-sensitive metals, and once a Ga_2O_3 oxide film is formed on the surface, it decreases the apparent surface tension of the droplet. As shown in Figure 3b, after the formation of static pendant-drop exposed to the atmosphere, the surface tension of the droplet surface subjected to the oxidation gradually decreases and shows an exponential decay form, which is obviously closely related to the oxygen concentration of the droplet surface, i.e., the surface tension gradually decreases with the increase of surface oxygen concentration.

According to the melting point of GaInSnBiZn alloy, a simultaneous heater was designed, and assembled for the drop tube and the sample stage, as shown in Figure 4. Under the condition of maintaining a constant temperature of 80 °C, the volume of the droplet was measured by the sessile-drop method, and the mass of the sessile-drop was obtained in combination with an analytical balance (accuracy of 0.0001 g), and the density of the liquid GaInSnBiZn alloy was calculated to be 6.8413-6.8416 g/cm^3. The surface tension of GaInSnBiZn alloy was also determined by the continuous pendant-drop method, which was 545±5 mN/m, as shown in Figure 5a. When the droplets were exposed to atmosphere for a few seconds, the droplet profile shape changed significantly, as shown in Figure 5b, and the surface tension decreased significantly to 252±20 mN/m. In the order of oxidizability of the alloy composition Zn>Ga>In>Sn>Bi, it is possible that the decrease in surface tension after oxidation is related to the formation of ZnO and Ga_2O_3.

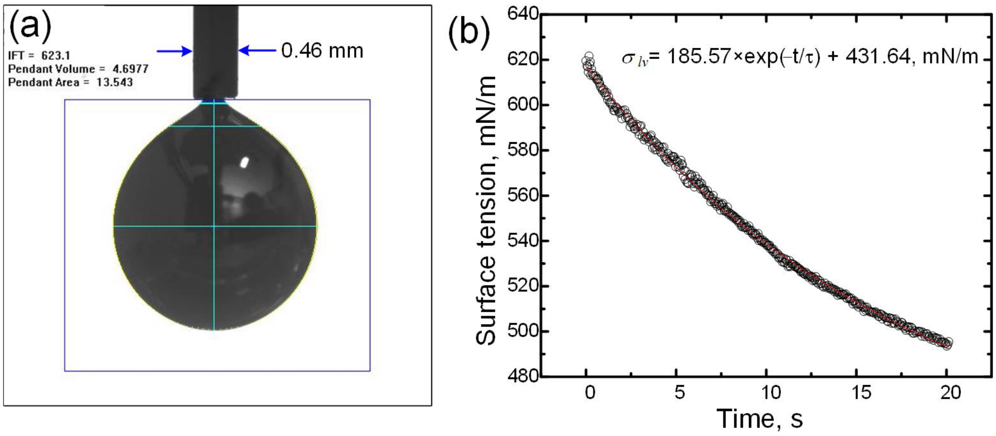

Figure 3. (a) Surface tension of E-GaIn alloy measured at 0.46 mm outside diameter of the drop tube; (b) Variation of surface tension with exposure time of liquid E-GaIn alloy

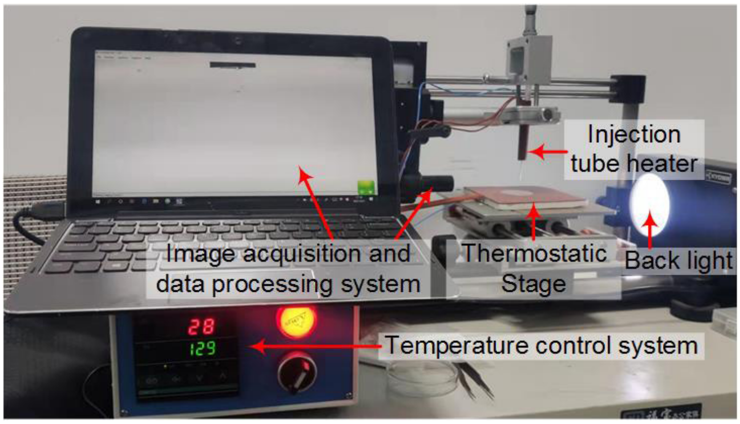

Figure 4. Surface tension measurement device after the introduction of heating and temperature control system

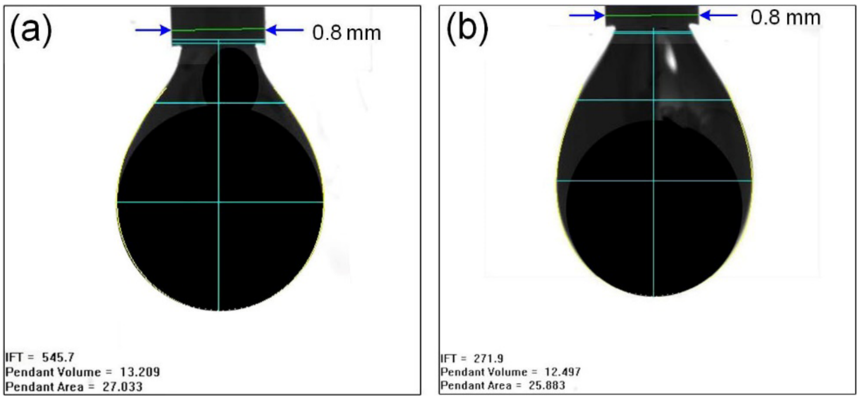

Figure 5. Surface tension of GaInSnBiZn alloy measured at 0.8 mm outside diameter of the drop tube. (a) instantaneous snap of pendant-drop; (b) pendant-drop after exposure air for several seconds

4. Surface Tension Analysis of Multi-component Alloys

For an ideal solution, the surface tension can be expressed as,

$$\sigma^i = x_{Ga}\sigma_{Ga} + x_{In}\sigma_{In} + x_{Sn}\sigma_{Sn} + x_{Bi}\sigma_{Bi} + x_{Zn}\sigma_{Zn} \tag{1}$$

Where σ^i is the surface tension under ideal solution conditions, and x_i is the molar fraction of each component. Since the equal atomic proportions are mixed as shown in Table 2, σ^i = 597.8 mN/m under ideal solution conditions, density ρ^i is 7.341 g/cm^3, and molar mass M^i is 115.522 g/mol.

Based on the assumption of high entropy alloy formation, all atoms are randomly distributed under ideal conditions, i.e., the solution formed is an ideal solution. Obviously, the measured data of surface tension and density indicate that the liquid GaInSnBiZn alloy is not an ideal solution, and the existence of local clusters or segregation within the liquid phase makes the apparent value of surface tension deviate from the ideal solution model.

Table 2. Surface tension (σ_i), density (ρ), molar mass (M_i) and molar area (Ω_i) of pure metal at melting point

	Ga*	In	Sn	Bi	Zn
σ_i^0, mN/m	713	556	560	378	782
ρ_i, g/cm^3	6.07	7.03	6.98	10.05	6.575
M_i, g/mol	69.72	114.8	118.7	209.0	65.39
Ω_i, m^2/mol	4.74×10^4	5.78×10^4	5.91×10^4	7.09×10^4	4.04×10^4

*Ga is the surface tension and density at 80 °C

Currently, most of the theoretical models for surface tension of multivariate (quaternary or even quintuplet) alloys are predicted based on binary alloy system models, such as the Guggenheim model [13], the GSM (universal solution) model [14] and the Butler model [15].

The Guggenheim model [13] is expressed as,

$$e^{-(\frac{\sigma\Omega}{RT})} = \sum_{i=5}^{5} e^{-(\frac{\sigma_i\Omega_i}{RT})} \tag{2}$$

Where Ω_i is the molar area of a single component, can be calculated from $\Omega_i = fN_a^{1/3}V_i^{2/3}$, where f is a structure factor (equals 1.091), N_a is Avogadro constant and V_i is the molar volume ($V_i = M_i/\rho_i$). Substituting the data in Table 2 yields a surface tension of 440 mN/m, which is obviously far from the surface tension obtained from the actual measurement.

The Butler model [15] is expressed as,

$$\sigma = \sigma_i + \frac{RT}{\Omega_i}\ln\frac{c}{1+(c-1)x_i^b} \tag{3}$$

where $c = e^{-(\frac{\Omega_i\left(\sigma_2^0-\sigma_1^0\right)}{RT})}$.

Table 3. Surface tension and excess surface tension of binary alloys mixed at 1:1 atomic ratio

Binary systems	Ideal solution, mN/m	Belton model, mN/m	σ_{ij}^E, mN/m
Ga-In	635	592	−43
Ga-Sn	637	595	−42
Ga-Bi	546	414	−132
Ga-Zn	748	739	−9
In-Zn	669	597	−72
In-Sn	558	558	0
In-Bi	467	409	−58
Sn-Bi	469	409	−60
Sn-Zn	671	600	−71
Bi-Zn	580	417	−163

The GSM model [14] can be expressed as,

$$\sigma^E = \frac{x_1x_2}{X_1X_2}\sigma_{1,2}^E + \frac{x_1x_3}{X_1X_3}\sigma_{1,3}^E + \frac{x_1x_4}{X_1X_4}\sigma_{1,4}^E + \frac{x_1x_5}{X_1X_5}\sigma_{1,5}^E + \frac{x_2x_3}{X_2X_3}\sigma_{2,3}^E + \frac{x_2x_4}{X_2X_4}\sigma_{2,4}^E + \frac{x_2x_5}{X_2X_5}\sigma_{2,5}^E + \frac{x_3x_4}{X_3X_4}\sigma_{3,4}^E + \frac{x_3x_5}{X_3X_5}\sigma_{3,5}^E + \frac{x_4x_5}{X_4X_5}\sigma_{4,5}^E \tag{4}$$

Where σ^E is the excess surface tension, i.e., the partial surface tension that deviates from the ideal solution, $\sigma^E = \sigma - \sigma^i$. x_i is the concentration of element i in the five-element system, and X_i is the concentration of element i in the binary system. Since the alloy is mixed with equal atomic ratio, x_i =0.2 and X_i =0.5, σ^E =−104 mN/m can be obtained from the data in Table 3, and the surface tension σ predicted by the model is 493.8 mN/m, which again deviates from the measured value.

Nevertheless, the predictions of the above models indicate that the actual surface tension of GaInSnBiZn should have a negative deviation with respect to the ideal solution, i.e., the actual surface tension should be less than the surface tension obtained from the ideal solution model. Since the alloy is mixed with equal atomic ratios, the surface tension of the alloy is 533 mN/m by taking the average value of the surface obtained from the Belton model, so the Butler model (or Belton model) is closer to the measured value.

In addition, according to the Butler model, the concentration of elements on the surface can be expressed as,

$$x_i^s = x_i^b \exp\left[\frac{(\sigma-\sigma_i)\Omega_i - 0.17\Delta S_i^E T}{RT}\right] \tag{5}$$

In high entropy alloys, the free energy of alloy formation is mainly derived from the contribution of entropy, so the excess free energy of the bulk phase in the above equation is replaced by $\Delta S_i^E T$. It can be concluded that the larger the contribution of each element to the excess entropy, the smaller its concentration at the surface and the smaller its contribution to the surface tension. The surface tension of the alloy is positive compared to the surface tension of the pure substance of each element, only the excess surface tension of the Bi element, where $x^s_{\mathrm{Ga}} + x^s_{\mathrm{In}} + x^s_{\mathrm{Sn}} + x^s_{\mathrm{Bi}} + x^s_{\mathrm{Zn}} = 1$. The surface concentration of all the elements except Bi is less than the nominal concentration of the bulk phase 0.2, which means that the surface concentration of Bi is much larger than the nominal concentration of the bulk phase ($x^s_{\mathrm{Bi}} > 0.2$), and thus the contribution of Bi to the entropy of alloy formation is minimal.

5. Conclusions

(1) The intrinsic surface tension of GaInSnBiZn high-entropy alloy at 80 °C was determined by the continuous pendant-drop method as 545±5 mN/m. The surface tension of the alloy decreased significantly with the formation of the surface oxide film.

(2) The Guggenheim model, GSM model, and Butler model were applied to calculate the surface tension of GaInSnBiZn high-entropy alloy, among which the calculation results obtained from the Butler model are in good agreement with the experimental data. Combined with the Butler model, the surface concentration of Bi is much higher than the other components and contributes the most to the surface tension, however, it contributes the least to the entropy of alloy formation.

Credit Authorship Contribution Statement

Shirong Zhu: Methodology, Writing, original draft. Lu Liu: Data analysis, Editing. Qiaoli Lin: Supervision, Work idea, Revision.

Declaration of Competing Interest

The authors declare that they have no known competing financial interests or personal relationships that could have appeared to influence the work reported in this paper.

Funding

This work is supported by National Natural Science Foundation of China (No. 52165044).

Conflict of Interest

No conflict of interest exists to declare.

References

[1] Wang, X., Guo, R., Liu, J., 2019. Liquid metal based soft robotics: materials, designs, and applications. Advanced Materials Technologies. 4, 1800549.

[2] Zhao, X., Xu, S., Liu, J., 2017. Surface tension of liquid metal: role, mechanism and application. Frontiers in Energy. 11, 535-567.

[3] Joo, S.H., Kato, H., Jang, M.J., Moon, J., Kim, E.B., Hong, S.J., Kim, H.S., 2017. Structure and properties of ultrafine-grained CoCrFeMnNi high-entropy alloys produced by mechanical alloying and spark plasma sintering. Journal of Alloys and Compounds. 698, 591-604.

[4] Zhang, Y., Zuo, T.T., Tang, Z., Gao, M.C., Dahmen, K.A., Liaw, P.K., Lu, Z.P., 2014. Microstructures and properties of high-entropy alloys. Progress in Materials Science. 61, 1-93.

[5] Ye, Y.X., Liu, C.Z., Wang, H., Nieh, T.G., 2018. Friction and wear behavior of a single-phase equiatomic TiZrHfNb high-entropy alloy studied using a nanoscratch technique. Acta Materialia. 147, 78-89.

[6] Yan, X., Zhang, Y., 2020. Functional properties and promising applications of high entropy alloys. Scripta Materialia. 187, 188-193.

[7] Fujii, H., Matsumoto, T., Nogi, K., 2000. Analysis of surface oscillation of droplet under microgravity for the determination of its surface tension. Acta Materialia. 48, 2933-2939.

[8] Przyborowski, M., Hibiya, T., Eguchi, M., Egry, I., 1995. Surface tension measurement of molten silicon by the oscillating drop method using electromagnetic levitation. Journal of Crystal Growth. 151, 60-65.

[9] Iida, T., Guthrie, R., 1988. The Physical Properties of Liquid Metals. UK: Oxford University Press.

[10] Ding, Y., Zeng, M., Fu, L., 2020. Surface chemistry of gallium-based liquid metals. Matter. 3, 1477-1506.

[11] Cui, Y., Ishihara, S., Liu, X., Shirong, Ohnuma, I., Kainuma, R., Ohtani, H., Ishida, K., 2002. Thermodynamic calculation of phase diagram in the Bi-In-Sb ternary system. Materials Transactions. 43, 1879-1886.

[12] Ren, L., Xu, X., Du, Y., Kalantar-Zadeh, K., Dou, S.X., 2020. Liquid metals and their hybrids as stimulus–responsive smart materials. Materials Today. 34, 92-114.

[13] Guggenheim, E.A., 1945. Statistical thermodynamics of the surface of a regular solution. Transactions of the Faraday Society. 41, 150-156.

[14] Yan, L., Zheng, S., Ding, G., Xu, G., Qiao, Z., 2007. Surface tension calculation of the Sn–Ga–In ternary alloy. Calphad. 31(1), 112-119.

[15] M'chaar, R., Sabbar, A., El Moudane, M., Ouerfelli, N., 2020. A survey of surface tension, molar volume and density for Sn–Ag–Cu–Bi–Sb quinary alloys as lead-free solders. Philosophical Magazine. 100, 1415-1438.